Analysis of the flexural mode response of a novel trimaran by segmented model test

Abstract

A novel ship concept design is significantly an "adhoc" process. In the preliminary design stage of novel vessels, it is very important to be able to develop an initial estimate of the effects of stiffness and mass distribution on the longitudinal flexural natural frequencies due to different general arrangements in still water at zero speed to satisfy design specifications. For new emerging designs, this estimate has to be made based on a model test. The experiments should also be planned so that scales effects and other features that are not present in full scale case, are minimized. A model with a length of 1.5 meter has been selected. The model was cut into four segments longitudinally and connected by a backbone beam with three elastic hinges joining the four segments. Wet vibration tests were conducted on the model, showed significant influences on the flexural natural frequencies through variations in stiffness and different mass distributions. The whipping frequency was calculated with four degrees of freedom theoretical model to compare with the experimental results. The theoretical model shows a good agreement with the experimental results.

Karim Akbari Vakilabadi[a]
Mohammad Reza Khedmati[b]
Habiballah Sayyari[c]

[a,b]Department of Marine Technology, Amirkabir University of Technology, Tehran, Iran
[c]Supreme National Defense University, Tehran, Iran

[b]Corresponding author:
khedmati@aut.ac.ir

1 INTRODUCTION

Marine vehicles with speeds above 30-35 knots which have recently been used primarily for both passenger transport and military applications are limited to high-speed monohulls and Multihulls. High forward speeds, complex structural outlines and the use of novel materials make the analysis of these vessels more challenging than conventional ships. During the last few years, there has been an increasing interest in the application of high speed multihull ships for military applications. When the high speed vessel concepts are up scaled, some new problems arise. The global hydrodynamic loads depend both on the ship's rigid body motions and its elastic deformation. These hydro-

elastic effects can be of particular importance for large high speed vessels. Springing is one of the challenges in ship-shape vessels. High speed and low rigidity are two features of a ship which generally increase the springing problems. The springing phenomenon may not influence the extreme structural responses, but the fatigue damage could be significantly increased (Friis-Hansen et al., 1995).

Hydroelasticity can be significant not only for steady state responces but also for those of the transient type. The flexibility of the structure in the area of slamming impact can influence the total slamming load (Kvalsvold, 1994), and the overall stiffness of the vessel's structure is important for global (whipping) responses. Ship classification societies have traditionally predicted the structural loads of ships using an empirical approach based on experience with previous vessels in contrast to an experimental analysis of the wave induced loads, Thomas et al. (2003a). Segmented monohull models have been traditionally developed to measure motions and loads at low Froude numbers as the work reported by Gerritsma et al. (1964) and Lloyd et al. (1979). This was followed by the evolution of low Froude number hydroelastic segmented models designed to replicate the whipping response of a full-scale vessel in addition to measuring motions and loads for the validation of numerical simulations, McTaggart et al. (1997). Dessi et al. (2005) have developed an elastically scaled high-speed monohull model used to measure dynamic loads and to replicate the modal response of the full-scale vessel with experimental results showing good correlation with finite element theory for dry tests in air. Kapsenberg et al. (2003) investigated a similar monohull model with an emphasis on slam loads and mathematically simulating whipping responses. Despite the extensive works have been conducted on the prediction and measurement of dry modal frequencies there is a lack of knowledge in validation of the theoretical wet modal frequency with the experimental wet modal frequency.

The model should be as simple as possible in order to provide easy and accurate measurements, and to keep production costs and time within reasonable limits. At the same time it should be sufficiently realistic for final calculations to be of practical values. Similarly, the model should be flexible enough to produce easily measurable hydroelastic responses, but not so flexible that qualitatively unrealistic phenomena occur. As discussed by Maeda (1991), flexible ship models can be constructed by different principles. The seakeeping Committee of 17th ITTC (ITTC 1984) also discusses various aspects of flexible model tests. A logical approach is to make the model continuously elastic (Watanabe et al., 1988). By this approach the stiffness distribution resembles a real ship, but it is difficult to adjust the stiffness once the model was produced. Alternatively, one can divide the ship hull into segments and connect the segments with a beam, or backbone, that has the proper stiffness. The backbone could be continuously elastic (Riska, 1994), or it could consist of stiff parts that are connected by elastic hinges (Troesch, 1984). Wereldsma (1974) has also proposed to use a completely stiff backbone. In the present experiments a novel wave piercer bow trimaran was utilized. The model was originially completely rigid, and the only practical way of making it flexible was to cut it into three segments. A rigid backbone frame with three elastic hinges was selected. According to variety of mass distribution due to different general arrangement, the vessels flexibility could be adjusted by changing the hinge geometry.

This paper presents the results on investigating the hydroelastic whipping response of a segmented wave piercer bow trimaran model with an emphasis on developing a theoretical model to

predict the wet modal frequency which is validated with experiments. The effect of model stiffness and an weight distributionon the measured flexural response has been studied. A theoretical model of a four degree of freedom system using an theoretical hydrodynamic added mass was developed to predict the wet modal frequency of the model as a function of stiffness and mass distributions.

2 SELECTION OF MODEL WEIGHT DISTRIBUTIONS BASED ON A PROTOTYPE VESSEL

Light warships are typical of volume-limited ships and it is these types which are most suited to the wider and more convenient deck spaces above the waterline that the multihull offers. A more complex investigation into the choice of hullform must be based on the required attributes of the ship, such as arrangement, speed and seakeeping. Multihulls provide a good and useful deck layout with a greater deck area per ton of displacement compared to monohulls. Arrangement is a crucial parameter that affectes the weight distribution in the model test.

Estimation and prediction of weight distribution is an essential task in the design phase of a vessel, and the accuracy of this work will be crucial for the success of the project. Weight distribution is based on required general arrangement according to vessel missions. Prediction-based design uses a set of user specifications for a certain class of ships to predict the rest of the weight distribution parameters. The prediction of ship weight distribution is performed with an statistical method and international classification rules.

In the early stages of designing new ships it is necessary to estimate the weight per unit length of the vessel to predict the initial weight and cost. One of the most important issues for design of military vessels is a number of equipment, structural integrity, navigation facilities, armament and etc. Novel vessels have to be designed considering the limitations caused by these design requirements. For select the several logical general arrangement, shall be provide some class specific data for vessels. Table 1 give detailed The Weight Distribution for some selected Navy ship classes are presented in Table 1.

Table 2 presents the technical specification of the model which is based on the weight distribution presented in table 1. The ship to model scale ratio was 80 which is suitable for the size of the towing tank facility. Three weight distributions based on various general arrangements were considered in this experiment. Ship Model is divided in 20 stations longitudinally and each permanent segment weight is calculated.

3 THEORETICAL BACKGROUND

Wave induced slamming that occurs on a vessel, subjects the structure to an impulse load that responds with modal excitation that is characteristic to the design of high-speed craft, Thomas et al. (2003b). An impulse loading applied to the bow in head seas most often excites the first longitudinal mode of vibration in the vertical plane. The flexural frequency that is experienced by a prototype vessel as a result of wave excitation and slamming may be scaled to a model scale by applying a constant dimensionless wave encounter frequency between prototype and model scale and deducing the model scale flexural frequency as a function of the full-scale frequency and the square root of the full-scale to model scale length ratio as given by:

Weight segment STN-STN	Weight Per Segment, lton				
	DD963V	DD963N	DD993	FF1052	FFG7
FWD-0	0	0	0	10.25	19.4
0-1	292.63	313.95	341.12	120.81	41.6
1-2	150.77	155.11	176.87	227.12	84.2
2-3	177.06	200.28	215.29	145.32	108.3
3-4	296.62	211.84	259.47	114.63	201.6
4-5	495.39	373.8	468.52	110.53	217.6
5-6	356.95	371.98	386.21	281.63	266.3
6-7	554.18	566.12	577.06	277.84	273.2
7-8	689.09	697.38	753.01	361.94	109.6
8-9	603.53	609.35	651.18	198.94	189.9
9-10	697.34	728.05	693.78	270.45	268.2
10-11	581.52	580.02	689.04	283.75	273.2
11-12	706.47	712.6	875.02	268.35	246
12-13	619.19	571.36	643.72	218.46	220.2
13-14	440.53	445.46	487.83	287.16	302.2
14-15	443.78	367.78	551.32	209.86	250.6
15-16	421.31	296.79	495.89	239.97	184.6
16-17	388.4	360.19	481.8	171.87	207.6
17-18	313.36	293.75	414.81	162.17	101.8
18-19	364.79	342.27	366.42	144.98	162.3
19-20	302.46	276.95	258.06	147.98	120.2
20-AFT	0	0.03	0	0	25.4
SUM	8895.37	8475.06	9786.42	4254.01	3874

Table 1: Weight Distribution for selected ship clases (US Navy Direction Of Commander, 2000).

| Particular	Prototype [m]	Model (1/80) [m]
Length overall	124	1.55
Length at waterline	123.2	1.54
Beam overall	21.776	27.22×10^{-2}
Beam at waterline	9.6	12×10^{-2}
Depth	11.776	14.72×10^{-2}
Draught	4.384	5.48×10^{-2}
Length of side hull	36	45×10^{-2}
Beam of side hull	2.36	2.95×10^{-2}
Depth of side hull	8.136	10.17×10^{-2}
Draft of side hull	74.4	0.93×10^{-2}
Clearance between centerline of main and side hull	9.7	12.125×10^{-2}
Displacement	2248.81Tonne	4.39×10^{-3}

Table 2: Main particulars of prototype trimaran and its scaled model.

$$w_m = w_f \sqrt{\frac{l_f}{l_m}}$$

where

w_m = model scale modal frequency, w_f = full-scale modal frequency, l_f = full-scale length of vessel, l_m = model scale length. It is therefore possible to achieve the whipping frequency at model scale by scaling the full-scale frequency and designing the model with the capability of achieving a modal response that replicates the flexural dynamics of the full-scale vessel. Although the segmented model concept is an approximation of the full-scale vessel structural response, it facilitates a practical simulation of the whipping phenomena observed on a full-scale vessel.

A four degree of freedom theoretical model was developed in order to predict the longitudinal bending frequency of the model as a function of the effective stiffness and mass distribution of the model. Figure 1 shows the four degree of freedom model consists of a four rigid hull segments which are connected by three elastic hinges. The aft segment consists of aft main hull part and side hulls.
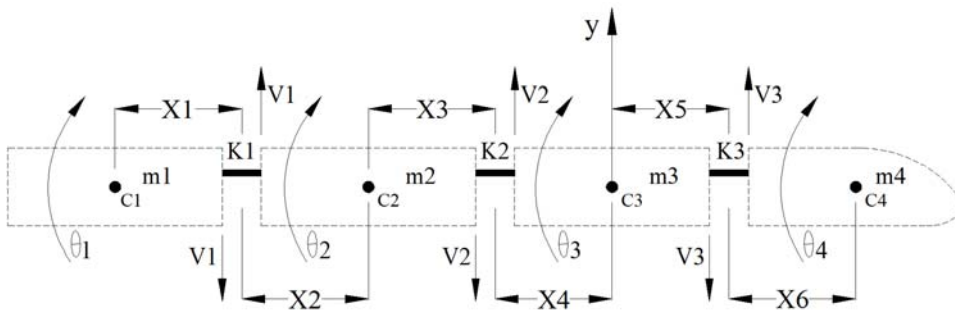
Figure 1: Four degrees of freedom system representing the segments of hull joined together with elastic hinges.

Let:

C1	centre of mass of segment-1	θ	rotation of hull segment
C2	centre of mass of segment-2	m	total mass
C3	centre of mass of segment-3	m_1	mass of segment 1
C4	centre of mass of segment-4	m_2	mass of segment 2
X_1	distance from K_1 to centre of mass of segment-1	m_3	mass of segment 3
X_2	distance from K_1 to centre of mass of segment-2	m_4	mass of segment 4
X_3	distance from K_2 to centre of mass of segment-2	K_1	stiffness of torsion spring-1
X_4	distance from K_2 to centre of mass of segment-3	K_2	stiffness of torsion spring-2
X_5	distance from K_3 to centre of mass of segment-3	K_3	stiffness of torsion spring-3
X_6	distance from K_3 to centre of mass of segment-4	V	shear force
I_1	moment of inertia of segment-1	I_2	moment of inertia of segment-2
I_3	moment of inertia of segment-3	I_4	moment of inertia of segment-4
y	vertical displacement		

The equations of motion representing this four degree of freedom system are

$$m_1\left(\ddot{y} + x_1\ddot{\theta}_1 + x_2\ddot{\theta}_2 + x_3\ddot{\theta}_2 + x_4\ddot{\theta}_3\right) = -V_1 \tag{1}$$

$$m_2\left(\ddot{y} + x_3\ddot{\theta}_2 + x_4\ddot{\theta}_3\right) = V_1 - V_2 \tag{2}$$

$$m_3\ddot{y} = V_2 - V_3 \tag{3}$$

$$m_4\left(\ddot{y} - x_6\ddot{\theta}_4 - x_5\ddot{\theta}_3\right) = V_3 \tag{4}$$

$$V_1 x_1 - K_1\left(q_1 - q_2\right) = I_1\ddot{q}_1 \tag{5}$$

$$K_1\left(q_1 - q_2\right) - K_2\left(q_2 - q_3\right) + V_1 x_2 + V_2 x_3 = I_2\ddot{q}_2 \tag{6}$$

$$K_2\left(q_2 - q_3\right) - K_3\left(\theta_3 - \theta_4\right) + V_2 x_4 + V_3 x_5 = I_3\ddot{\theta}_3 \tag{7}$$

$$V_3 x_6 - K_3\left(\theta_4 - \theta_3\right) = I_4\ddot{\theta}_4 \tag{8}$$

By substituting equation (1) in equation (2) we get V_2,

$$V_2 = m_1\left(\ddot{y} + x_1\ddot{\theta}_1 - x_2\ddot{\theta}_2 + x_3\ddot{\theta}_2 + x_4\ddot{\theta}_3\right) - m_2\left(\ddot{y} + x_3\ddot{\theta}_2 - x_4\ddot{\theta}_3\right) \tag{9}$$

Then:

$$\ddot{y} = \frac{-m_1 x_1\ddot{\theta}_1 - \left(m_1 x_2 + m_1 x_3 + m_2 x_3\right)\ddot{\theta}_2 - \left(m_1 x_4 + m_2 x_4 - m_4 x_5\right)\ddot{\theta}_3 + m_4 x_6\ddot{\theta}_4}{m}$$

By substituting equation (4) and equation (9) in equation (3) $\ddot{y}$ is obtained and by Eliminating $\ddot{y}$ from (6), (7) and (8) and

$$\begin{aligned}
&\left(-m_1 x_1\frac{m_4 x_4}{m}\right)\ddot{\theta}_4 + \left(-m_1 x_1 x_4 - m_1 x_1\frac{m_2 x_4 - m_4 x_5 - m_1 x_4}{m}\right)\ddot{\theta}_3 \\
&+\left(-m_1 x_1\frac{m_1 x_2 - m_1 x_3 - m_2 x_3}{m} - m_1 x_1 x_3 + m_1 x_1 x_2\right)\ddot{\theta}_2 + \left(m_1 x_1\frac{m_1 x_1}{m} - m_1 x_1 x_1 - I_1\right)\ddot{\theta}_1 - K_1\left(\theta_1 - \theta_2\right) = 0
\end{aligned} \tag{10}$$

$$\begin{aligned}
&-m_1 x_2\left(\frac{m_4 x_4}{m}\ddot{\theta}_4 + \frac{m_2 x_4 - m_4 x_5 - m_1 x_4}{m}\ddot{\theta}_3 + \frac{m_1 x_2 - m_1 x_3 - m_2 x_3}{m}\ddot{\theta}_2 - \frac{m_1 x_1}{m}\ddot{\theta}_1 + x_1\ddot{\theta}_1 - x_2\ddot{\theta}_2 + x_3\ddot{\theta}_2 + x_4\ddot{\theta}_3\right) \\
&-m_1 x_3\left(\frac{m_4 x_4}{m}\ddot{\theta}_4 + \frac{m_2 x_4 - m_4 x_5 - m_1 x_4}{m}\ddot{\theta}_3 + \frac{m_1 x_2 - m_1 x_3 - m_2 x_3}{m}\ddot{\theta}_2 - \frac{m_1 x_1}{m}\ddot{\theta}_1 + x_1\ddot{\theta}_1 - x_2\ddot{\theta}_2 + x_3\ddot{\theta}_2 + x_4\ddot{\theta}_3\right) \\
&-m_2 x_3\left(\frac{m_4 x_4}{m}\ddot{\theta}_4 + \frac{m_2 x_4 - m_4 x_5 - m_1 x_4}{m}\ddot{\theta}_3 + \frac{m_1 x_2 - m_1 x_3 - m_2 x_3}{m}\ddot{\theta}_2 - \frac{m_1 x_1}{m}\ddot{\theta}_1 + x_3\ddot{\theta}_2 - x_4\ddot{\theta}_3\right) \\
&+K_1\left(\theta_1 - \theta_2\right) - K_2\left(\theta_2 - \theta_3\right) = I_2\ddot{\theta}_2
\end{aligned} \tag{11}$$

$$\begin{aligned}
&\left(-m_1 x_4\frac{m_4 x_4}{m} - m_2 x_4\frac{m_4 x_4}{m} + m_4 x_5\frac{m_4 x_4}{m} - m_4 x_5 x_6\right)\ddot{\theta}_4 + \left(-I_3 - m_1 x_4\frac{m_2 x_4 - m_4 x_5 - m_1 x_4}{m} - m_1 x_4 x_4\right. \\
&-m_2 x_4\frac{m_2 x_4 - m_4 x_5 - m_1 x_4}{m} + m_2 x_4 x_4 + m_4 x_5\frac{m_2 x_4 - m_4 x_5 - m_1 x_4}{m} + m_4 x_5 x_5\Big)\ddot{\theta}_3 + \left(-m_1 x_4\frac{m_1 x_2 - m_1 x_3 - m_2 x_3}{m}\right. \\
&+m_1 x_4 x_2 - m_1 x_4 x_3 - m_2 x_4\frac{m_1 x_2 - m_1 x_3 - m_2 x_3}{m} - m_2 x_4 x_3 + m_4 x_5\frac{m_1 x_2 - m_1 x_3 - m_2 x_3}{m}\Big)\ddot{\theta}_2 + \left(m_1 x_4\frac{m_1 x_1}{m}\right. \\
&-m_1 x_4 x_1 + m_2 x_4\frac{m_1 x_1}{m} - m_4 x_5\frac{m_1 x_1}{m}\Big)\ddot{\theta}_1 + K_2\left(\theta_2 - \theta_3\right) + K_3\left(\theta_4 - \theta_3\right) = 0
\end{aligned} \tag{12}$$

$$\left(-I_4 + m_4 x_6 \frac{m_4 x_4}{m} - m_4 x_6 x_6\right)\ddot{\theta}_4 + \left(m_4 x_6 \frac{m_2 x_4 - m_4 x_5 - m_1 x_4}{m} + m_4 x_6 x_5\right)\ddot{\theta}_3$$
$$+ \left(m_4 x_6 \frac{m_1 x_2 - m_1 x_3 - m_2 x_3}{m}\right)\ddot{\theta}_2 + \left(-m_4 x_6 \frac{m_1 x_1}{m}\right)\ddot{\theta}_1 - K_3\left(\theta_4 - \theta_3\right) = 0 \tag{13}$$

Considering $\ddot{\theta}_i = -\omega_n^2 \theta_i$ results with the formulation of the following matrix

$$\begin{bmatrix} a_{11} & a_{12} & a_{13} & a_{14} \\ a_{21} & a_{22} & a_{23} & a_{24} \\ a_{31} & a_{32} & a_{33} & a_{34} \\ a_{41} & a_{42} & a_{43} & a_{44} \end{bmatrix} \begin{bmatrix} \theta_1 \\ \theta_2 \\ \theta_3 \\ \theta_4 \end{bmatrix} = 0 \tag{14}$$

where

w_n : natural frequency

$$a_{11} = \left(-m_1 x_1 \frac{m_1 x_1}{m} + m_1 x_1 x_1 + I_1\right)\omega_n^2 - K_1$$

$$a_{12} = \left(m_1 x_1 \frac{m_1 x_2 - m_1 x_3 - m_2 x_3}{m} + m_1 x_1 x_3 - m_1 x_1 x_2\right)\omega_n^2 + K_1$$

$$a_{13} = \left(m_1 x_1 x_4 + m_1 x_1 \frac{m_2 x_4 - m_4 x_5 - m_1 x_4}{m}\right)\omega_n^2$$

$$a_{14} = \left(m_1 x_1 \frac{m_4 x_4}{m}\right)\omega_n^2$$

$$a_{21} = a_{12}$$
$$a_{31} = a_{13}$$
$$a_{41} = a_{14}$$

$$a_{22} = \left[I_2 + m_1 x_2\left(\frac{m_1 x_2 - m_1 x_3 - m_2 x_3}{m}\right) + m_1 x_2 x_3 - m_1 x_2 x_2 + m_1 x_3 \frac{(m_1 x_2 - m_1 x_3 - m_2 x_3)}{m}\right.$$
$$\left. + m_1 x_3 x_3 - m_1 x_3 x_2 + m_2 x_3 \frac{(m_1 x_2 - m_1 x_3 - m_2 x_3)}{m} + m_2 x_3 x_3\right]\omega_n^2 - (K_1 + K_2)$$

$$a_{23} = \left[m_1 x_2 x_4 + m_1 x_2 \frac{(m_2 x_4 - m_4 x_5 - m_1 x_4)}{m} + m_1 x_3 \frac{(m_2 x_4 - m_4 x_5 - m_1 x_4)}{m}\right.$$
$$\left. + m_1 x_3 x_4 + m_2 x_3 \frac{(m_2 x_4 - m_4 x_5 - m_1 x_4)}{m} - m_2 x_3 x_4\right]\omega_n^2 + K_2$$

$$a_{24} = \left(m_1 x_2 \frac{m_4 x_4}{m} + m_1 x_3 \frac{m_4 x_4}{m} + m_2 x_3 \frac{m_4 x_4}{m}\right)\omega_n^2$$

$$a_{32} = a_{23}$$
$$a_{42} = a_{24}$$

$$a_{33} = \left[I_3 + m_1 x_4 \frac{(m_2 x_4 - m_4 x_5 - m_1 x_4)}{m} + m_1 x_4 x_4 + m_2 x_4 \frac{(m_2 x_4 - m_4 x_5 - m_1 x_4)}{m} \right.$$

$$\left. -m_2 x_4 x_4 - m_4 x_5 \frac{(m_2 x_4 - m_4 x_5 - m_1 x_4)}{m} - m_4 x_5 x_5 \right] \omega_n{}^2 - (K_2 + K_3)$$

$$a_{34} = \left(m_1 x_4 \frac{m_4 x_4}{m} + m_2 x_4 \frac{m_4 x_4}{m} - m_4 x_5 \frac{m_4 x_4}{m} + m_4 x_5 x_6 \right) \omega_n{}^2 + K_3$$

$$a_{43} = a_{34}$$

$$a_{44} = \left(I_4 - m_4 x_6 \frac{m_4 x_4}{m} + m_4 x_6 x_6 \right) \omega_n{}^2 - K_3$$

Evaluating the determinant of the matrix defined in equation 14 and excluding the solution at zero frequency for rigid body motion leads to the theoretical values of the natural frequencies of the four degree of freedom mass-spring system for which the determinant is zero. Table 3 shows a summary of the parameters that were input to the theoretical model and Figure 2 shows the results of the matrix determinant as a function of frequency for the evaluation of the wet modal frequency response of the hydroelastic segmented ship model.

Variable	Length(mm)	Variable	Value	Variable	Value
x_1	260	m_1	1000 gr	K_3	3000 N/m
x_2	120	m_2	1000 gr	I_1	0.35 Kg.m^2
x_3	130	m_3	1350 gr	I_2	0.1 Kg.m^2
x_4	160	m_4	1000 gr	I_3	0.5 Kg.m^2
x_5	140	K_1	3000 N/m	I_4	0.3 Kg.m^2
x_6	140	K_2	3000 N/m		

Table 3: Summary of the input physical parameters to the four degrees of freedom theoretical model.

$$\det(A) = 10^9 \left(4.152\omega^8 + 616\omega^6 + 3200\omega^4 - 3.72 \times 10^5 \omega^2 \right) \tag{15}$$

$$4.152\omega^8 + 616\omega^6 + 3200\omega^4 - 3.72 \times 10^5 \omega^2 = 0 \tag{16}$$

It is observed from the results shown in Figure 2 that the wet modal frequency of the four degree of freedom system is 0 Hz for rigid body motion, 4.61Hz for the first longitudinal mode.

Figure 3 shows the model first longitudinal mode shape calculated for natural frequency.

4 MODEL DESCRIPTION

4.1 Hull Shape

The body plan of the hull and its outline are shown in figure 4 and 5 respectively. The length between perpendiculars is almost 1.5 meter. The vessel has a longitudinal symmetry body plan under the water line. A summary of the main particulars is given in table 2.
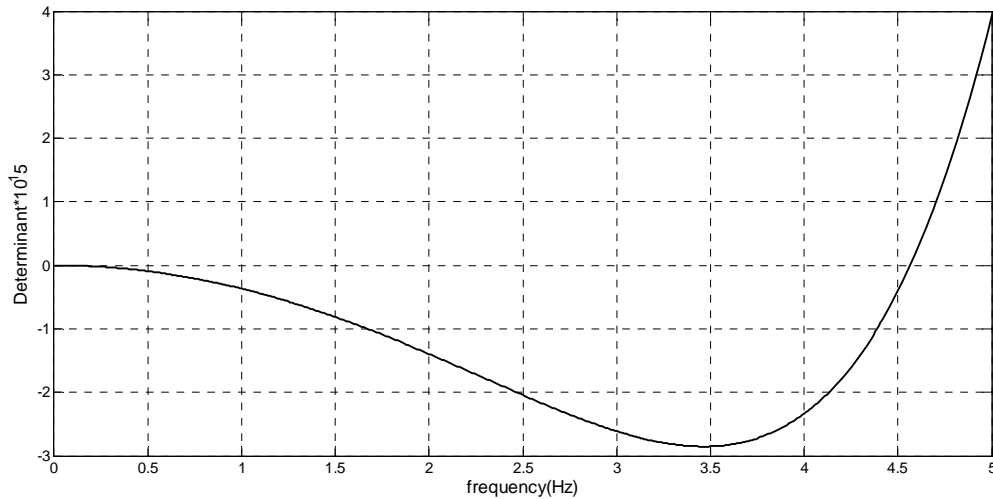
Figure 2: Matrix determinant of the four degrees of freedom mass-spring system for the theoretical evaluation of the wet flexural response frequency of the 1.5m test model based on the input parameters summarised in table 3.
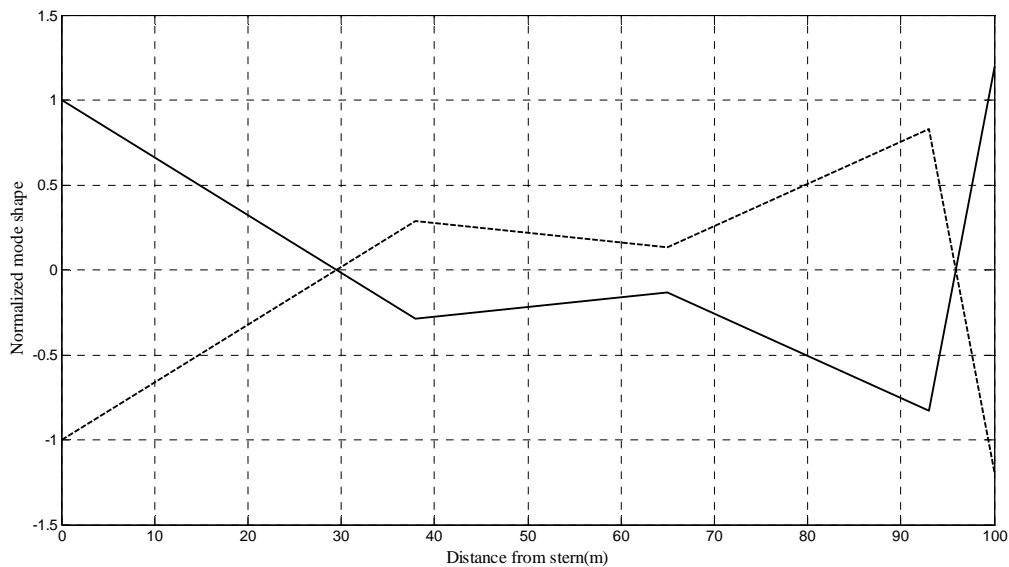
Figure 3: Hydroelastic segmented model normalised mode shape in still water and at zero speed at a natural bending frequency of 4.61Hz.

4.2 Stiffness distribution

The backbone frame is very stiff and the elastic hinges are located close to the gaps between the hull segments. There are three cut along the model length; one at the $0.25\,L_{pp}$ from FORE perpendicular, one at the midship and another at position of outriggers connect to main hull.
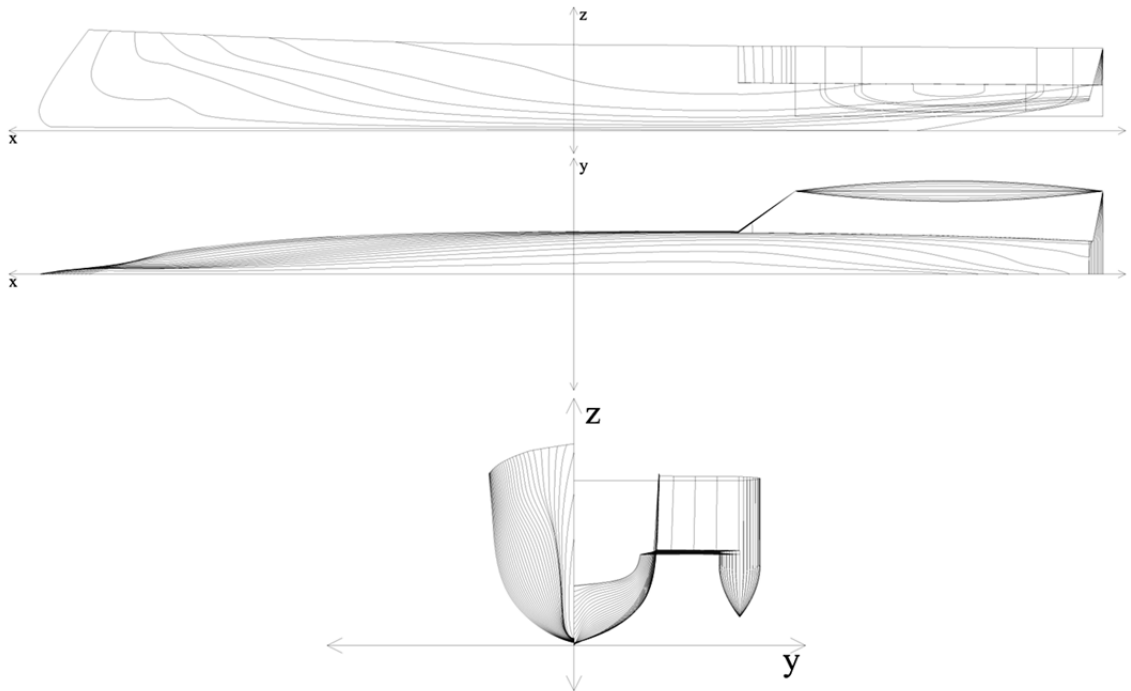
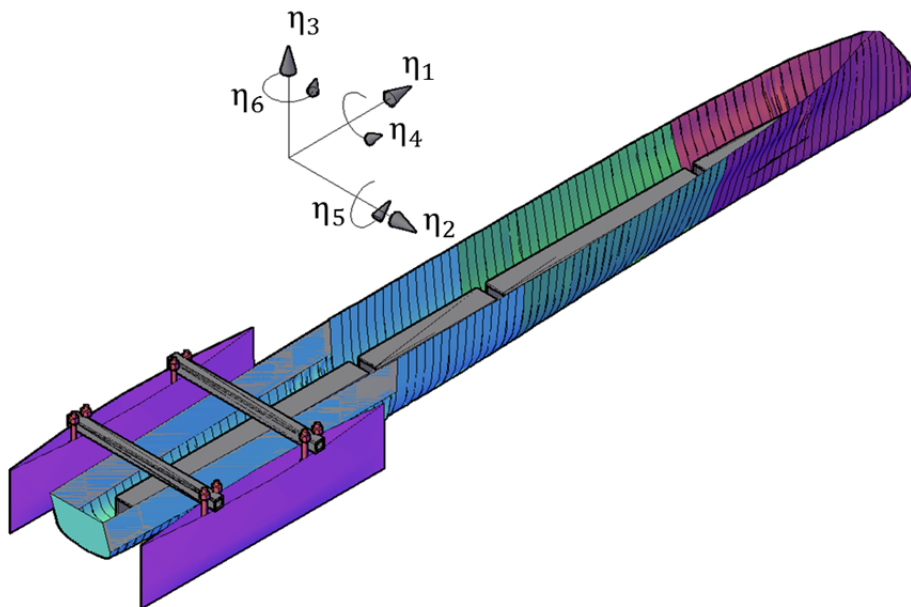**Figure 4:** Body plan of the trimaran model.

Figure 5: Outline of the trimaran model.

4.3 Mass Distribution

The model has a total mass of 4.35 kilograms, and the Pitch radius of gyration is 0.36. The origin of the coordinate system located at the center of gravity. The xy-plane is parallel to the calm water

surface when the ship is at rest at zero speed. Main contributions to the model's mass come from the hulls, which are made of fiber glass resin and backbone frame which is made of aluminum. The hull was cut longitudinally into three sections. Each rigid segment was attached to an aluminium square hollow section backbone beam. The segments of the model were joined together with three flexible elastic hinges that are interchangeable in order to vary the stiffness of the links. Separating the model into segregated compartments allowed the position and magnitude of ballast mass to be systematically located within the model to vary the configuration of ballast mass distribution according to three different general arrangements.

A schematic diagram of the elastic hinge is shown in Figure 6. The elastic hinge consists of a square hollow plug on either end that was connected at the center by a flexible link of square cross section. Either end of the elastic hinge was inserted into the aluminum SHS (32x32x1.5) beam and was joined together with bolts to produce a highly rigid connection. The cross section dimensions and length of the flexible link were varied in order to adjust the stiffness and flexibility of the connection. Aluminum alloy was selected as the most suitable material for the manufacture of the elastic hinges as it was sufficiently light and was found to provide adequate strength and stiffness. The elastic hinges were manufactured on a CNC programmable machine at the Amirkabir University of Technology.
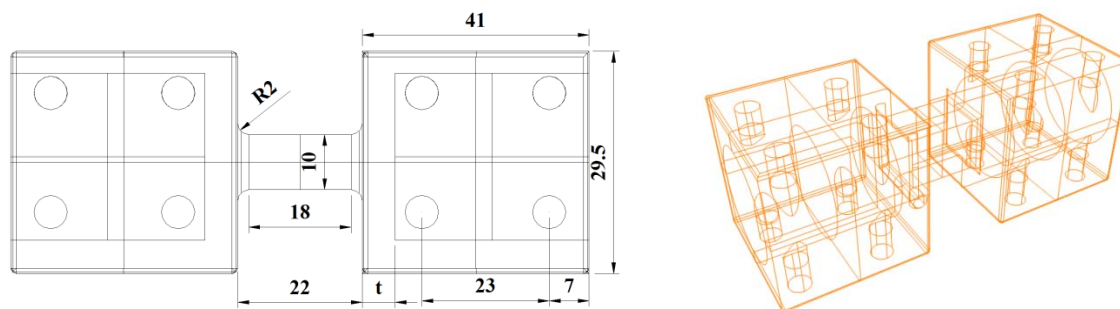
Figure 6: Elastic hinge built for the measurement of wave induced strains and the adjustment of stiffness.

Experimental bending tests were performed on a sample of elastic hinges with different wall thickness t, in order to investigate the effect of wall thickness and weight on the ultimate strength and stiffness. Four elastic hinge samples were manufactured with a design stiffness of 3000 Nm/rad and wall thickness t, of 4 mm, 8 mm, 12 mm and 15 mm. The end plug of each elastic hinge was fixed to a suitable mechanism in a cantilever arrangement. Experiment performed with compression testing machine and the loads were incremented until such stage the failure load and failure mechanism was physically identified (Figure 7).

With reference to Figure 8 it is obvious that increases in the wall thickness responded with increases in the ultimate strength of the elastic hinge. Physical experiments were therefore undertaken in order to identify the effects of wall thickness on the stiffness of the elastic hinge.

4.4 Data Acquisition

To measure the vertical acceleration a 3DM-GX1 instrument is used. Measured data were recorded digitally at sampling rate of 350 Hz.
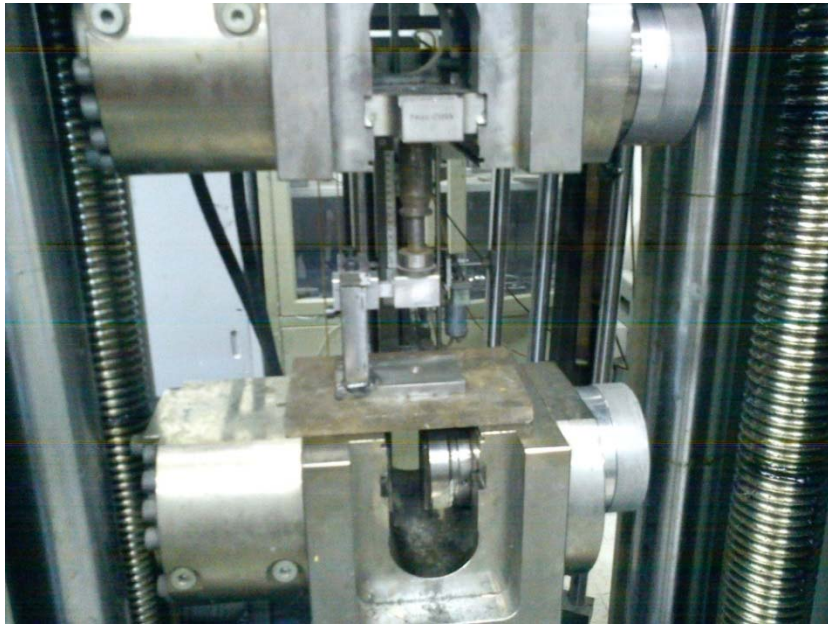
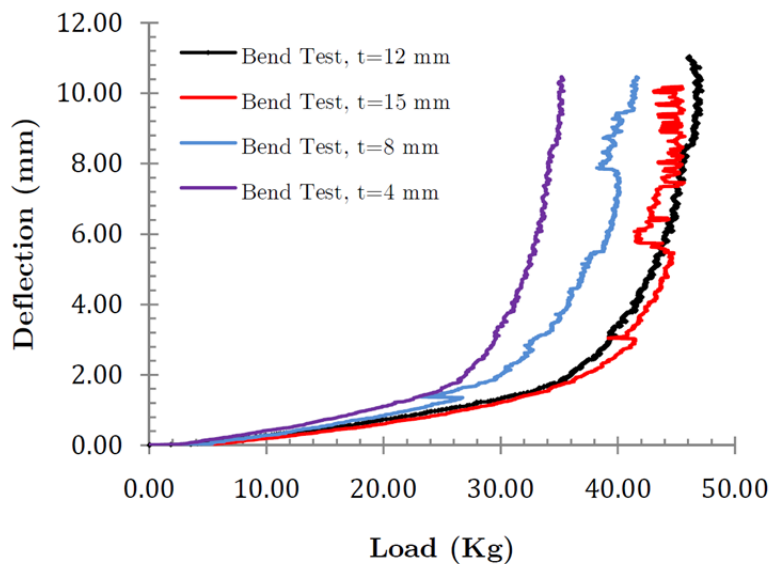**Figure 7:** Elastic hinge bending test by compression machine.

Figure 8: Deflections as a function of load for tests undertaken on the elastic hinges at a wall thickness of 4, 8, 12 and 15 mm.

5 TEST PROGRAM

5.1 Tests in air

In order to determine the eigen-frequencies, the corresponding mode shapes and the damping properties of the model, vibration tests were carried out. The model was suspended from four springs,

one at the midpoint of each segment, and vibrations were excited by giving it manual impulse force. Impulse force in different longitudinal locations will excite different mode shapes. Estimates of the damping levels and the eigen-frequencies, as well as an overview of mode shapes, were obtained by analyzing the signals from the microstrain. Useful information was obtained for the First mode by this method. The two springs from which the model was suspended, have eigen-frequencies that much smaller than those of the model therefore their influence on the measured frequencies could be neglected.

5.2 Test in water

Experiments were performed at towing tank of Marine Engineering Research Center, Sharif University of Technology. Towing Tank Particulars is presented in Table 4. Tests were undertaken in still water and at zero speed with the model unrestrained and free to respond with dominant motions in heave and pitch. An impulse load was applied by hand at the stern of the model in order to excite the longitudinal mode of vibration. The stern was selected as the most appropriate position as this produces the most reliable and reproducible signal response. Model accelerations were recorded using an accelerometer that was located at the different position of the model (Figure 9).
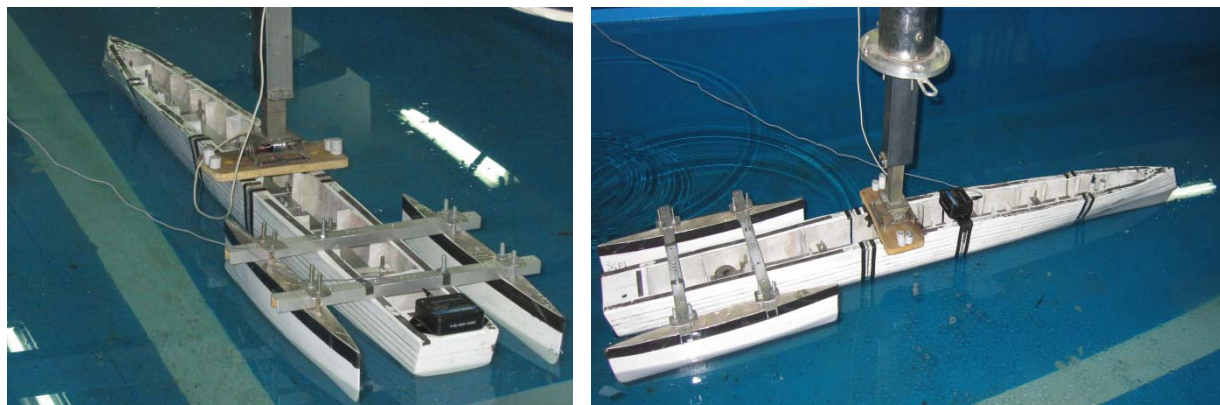
Figure 9: Measurements of the model accelerations by Microstrain.

Length×Width×Depth of the tank	Maximum Speed of carriage	Maximum acceleration of carriage	Towing System
25 × 2.5× 1.2 m	6 m/s	2 m/s^2	Electromotor (4 kW)

Table 4: Towing tank particulars.

The stiffness of the elastic hinge connecting the rigid hull segments was varied in order to investigate its effects on the flexural natural frequency response of the first longitudinal mode of vibration. Four elastic hinges of different stiffness were used to form the connection between the four rigid parts of the model. Bending tests were performed on the model by simply supporting it on either ends and applying a load at the connection point. It was found that the measured stiffness of both the hull and the backbone beam was considerably less than the theoretical stiffness of the elas-

tic hinge. It was observed that although the stiffness of the elastic hinge was increased the overall measured stiffness approached the stiffness of the hull. This was due to the inherent flexibility of the fibre glass hull and aluminium backbone beam causing significant bending between the mounting points across each segment of hull and is discussed in further detail by Jason Lavroff et al. (2006).

The modal frequency response of the model was also evaluated as a function of the ballast mass distribution. According to three different general arrangements, the ballast masses were located within the designated compartments of the model to produce three distinct mass distributions while maintaining a constant trim angle for each elastic hinge stiffness configuration. Essentially this enabled the variation of both the ballast mass distribution and the effective stiffness of the model in order to observe the effects on the whipping frequency response. Table 5 presents three general arrangement configurations implemented during trials conducted on the trimaran hydroelastic model.

G.A' s	Compartment number												
	1	2	3	4	5	6	7	8	9	10	11	12	13
1	-	-	60 gr	-	-	25 gr	-	-	-	-	140 gr	-	-
2	-	-	-	60 gr	-	-	-	25 gr	-	140 gr	-	-	-
3	-	-	60 gr	-	-	-	-	140 gr	-	-	25 gr	-	-
-	Segment 1			Segment 2				Segment 3		Segment 4			

Table 5: Model mass distribution according to General Arrangement (G.A).

A series of tests in calm water at zero speed are conducted on a novel Trimaran vessel in order to predict its Flexural Mode Response. There were altogether 42 test conditions. A brief summary of the tests is presented in Table 6 and Figure 9 shows a sample test.

General Arrangement	MicroStrain Positions				
	Pos1	Pos2	Pos3	Pos4	Pos5
GA1	√	√	√	√	√
GA2	√	√	√	√	√
GA3	√	√	√	√	√

Table 6: Testing matrix for Flexural Mode Response.

6 MODEL TEST RESULTS

The whipping response was clearly observed during all tests undertaken on the segmented model. Figure 10 displays a typical accelerometer response recorded on the trimaran model following an impulse load at the stern.

According to the power spectral analysis for a test case with an effective stiffness of 3000 Nm/rad, a ballast mass distribution corresponding to GA 1, the first longitudinal natural frequency is 3.1 Hz. The Difference between the measured frequency and the analytical solution is due to the configuration of AFT segment. In theoretical AFT segment was mono Hull and in experiment was three hulls.
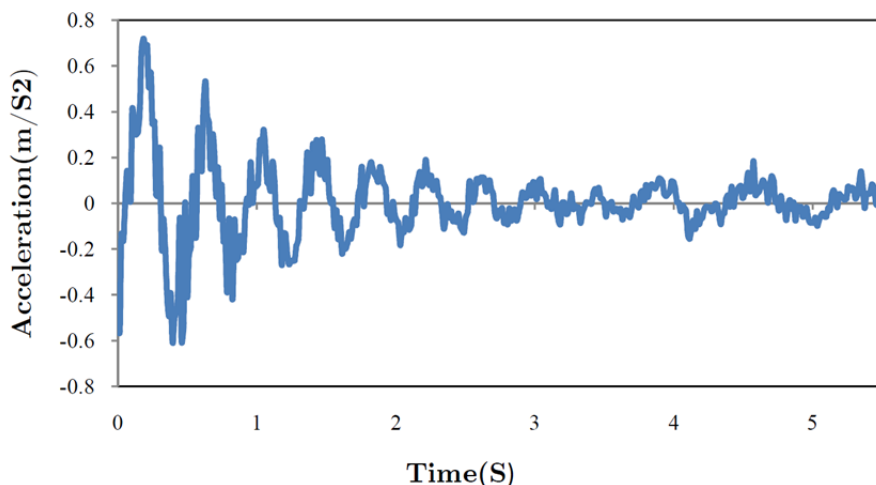
Figure 10: Whipping accelerations recorded at mid-ship of the experimental model.

7 CONCLUSIONS

A design methodology was developed to investigate the modal frequency of a trimaran ship model through the adjustment of stiffness with an elastic hinge and variety of general arrangements. These findings formulate an effective mechanism for attaining the natural frequency response of a segmented model for the purpose of replicating the whipping response of a full-scale vessel subject to slamming. It was shown that the full-scale whipping frequency could be scaled down to a model scale and through the adjustment of the appropriate parameters the target whipping frequency may be achieved.

A theoretical model was developed based on a four degree of freedom mass-spring system representing four rigid hull segments connected by a set of springs longitudinally. It was shown that the theoretical model gave accurate predictions of modal frequency when compared to experimental results based on the effective stiffness of the model. The validation of the theoretical model through experiments aids the on-going development of a future hydroelastic model. Because of the aft segment configuration the measured experimental natural frequency is different from the theoretical one.

References

Dessi, D., Mariani, R., Coppottelli, G., Rimondi, M., (2005). Experimental identification of wet bending modes with segmented model tests. 8th International Conference on Fast Sea Transportation, FAST '05.

Friis Hansen, P., Winterstein, S. R., (1995). Fatigue Damage in the Side Shells of Ships. Marine Structures Vol. 8: 631-555.

Gerritsma, J., Beukelman, W., (1964). The distribution of the hydrodynamic forces on a heaving and pitching shipmodel in still water. Fifth Symposium on naval hydrodynamics ship motions and drag reduction, 219–246.

Kapsenberg, G.K., Van't Veer, A.P., Hackett, J.P., Levadou, M.M.D., (2003). Aftbody Slamming and Whipping Loads. Transactions of the Society of Naval Architects and Marine Engineers 111: 213-231.

Kvalsvold, J., Faltinsen, O.M., (1995). Hydroelastic modeling of wetdeck slamming on multihukl vessels. Journal of Ship Research 39: 225-229.

Lavroff, J., Davis, M. R., Holloway, D. S., Thomas, G., (2006). Experimental Analysis of the Wet Flexural Mode Response of an NPL 6A Hydroelastic Segmented Model. 5th International Conference on High Performance Marine Vehicles, 8-10 November.

Lloyd, A.R.J.M., Brown, J.C., Anslow, J.F.W., (1979). Motions and loads on Ship Models in Regular Oblique Waves. Transactions of the Royal Institution of Naval Architects 122: 21-43.

Maeda, H., (1991). Modelling Techniques for dynamics of ships. Phil, Trans. R. Soc. London A 334: 304-317.

McTaggart, K., Datta, I., Stirling, A., Gibson, S., Glen, I., (1997). Motions and Loads of a Hydroelastic Frigate Model in Severe Seas. Transactions of the Society of Naval Architects and Marine Engineers 105: 427-453.

Riska, R., Kukkanen, T., (1994). Speed dependence of the natural modes of an elastically scaled ship model. hydroelasticity in marine technology, Rotterdam, The Netherlands, 157-168.

Thomas, G., Davis, M.R., Holloway, D.S., Roberts T.J., (2003a). Transient Dynamic Slam Response of Large High-speed Catamarans., 7th International Conference on Fast Sea Transportation, FAST '03.

Thomas, G., Davis, M.R., Holloway, D.S., Roberts, T.J., (2003b). The whipping vibration of large high-speed catamarans. Transactions of the Royal Institution of Naval Architects 145 A4: 13-29.

Troesch, A. W., (1984). Wave-induced hull vibrations: an experimental and theoretical study. Journal of Ship Research 28(2): 141-150.

US Navy Direction Of Commander, Naval Sea Systems Command, (2000). US Navy Salvage Engineer's Handbook, Volume 1. S0300-A8-Hbk-010.

Watanabe, I., Sawada, H., (1985). Effect of elastic responses to the longitudinal bending moment in two-directional irregular waves. J.S.N.A Japan 158.